Impact of aragonite saturation state changes on migratory pteropods

Steeve Comeau[1,2,*], **Jean-Pierre Gattuso**[1,2], **Anne-Marin Nisumaa**[1,2] **and James Orr**[3]

[1]*CNRS-INSU, Laboratoire d'Océanographie de Villefranche, BP 28, 06234 Villefranche-sur-Mer Cedex, France*
[2]*Université Pierre et Marie Curie-Paris 6, Observatoire Océanologique de Villefranche, 06230 Villefranche-sur-Mer, France*
[3]*LSCE/IPSL, Laboratoire des Sciences du Climat et de l'Environnement CEA-CNRS-UVSQ, F-91191 Gif-sur-Yvette Cedex, France*

Thecosome pteropods play a key role in the food web of various marine ecosystems and they calcify, secreting the unstable $CaCO_3$ mineral aragonite to form their shell material. Here, we have estimated the effect of ocean acidification on pteropod calcification by exploiting empirical relationships between their gross calcification rates ($CaCO_3$ precipitation) and aragonite saturation state Ω_a, combined with model projections of future Ω_a. These were corrected for modern model-data bias and taken over the depth range where pteropods are observed to migrate vertically. Results indicate large reductions in gross calcification at temperate and high latitudes. Over much of the Arctic, the pteropod *Limacina helicina* will become unable to precipitate $CaCO_3$ by the end of the century under the IPCC SRES A2 scenario. These results emphasize concerns over the future of shelled pteropods, particularly *L. helicina* in high latitudes. Shell-less *L. helicina* are not known to have ever existed nor would we expect them to survive. Declines of pteropod populations could drive dramatic ecological changes in the various pelagic ecosystems in which they play a critical role.

Keywords: ocean acidification; zooplankton; Arctic

1. INTRODUCTION

Since pre-industrial time, large quantities of carbon dioxide (CO_2) have been released into the atmosphere as a result of fossil-fuel burning and deforestation [1]. Atmospheric CO_2 concentrations have increased roughly exponentially from about 280 ppm in the eighteenth century to about 390 ppm today. The oceans have buffered this increase by taking up the equivalent of about one-fourth of anthropogenic CO_2 emissions [1–3]. As this extra CO_2 dissolves in sea water, it forms additional carbonic acid and reduces ocean pH. Since pre-industrial time, surface ocean pH has fallen by about 0.1 unit [4], and models project that under the IPCC IS92a scenario, there will be a further decline of 0.3–0.4 units by the end of the century [4]. Yet, ocean acidification does not only reduce ocean pH, but also reduces the carbonate ion concentrations and thus associated saturation states (Ω) of calcium carbonate. Models project that under the continuously increasing CO_2 emissions scenario, IPCC IS92a (approx. 790 ppm by the year 2100) [5], which is similar to the SRES A2 scenario, Southern Ocean surface waters begin to become undersaturated with respect to aragonite by the year 2050 [6]. In the Arctic Ocean, one model projects that such undersaturation will occur as early as 2016 during one month per year in

10 per cent of the Arctic [7]. Subsurface waters are also affected by ocean acidification. Models project that the aragonite saturation horizon (ASH; the interface between undersaturated waters below and supersaturated waters above) will move upward (shoal) throughout the ocean. In the Atlantic north of $50°$ N, models project that the ASH will shoal from 2600 to 115 m by the year 2100 under the IS92a scenario [6].

Reductions in pH and carbonate ion concentration may have an affect on some organisms and alter ecosystems. Previous studies demonstrate that some key calcifiers, such as coccolithophores [8], corals and coralline algae [9–11], molluscs [12] and echinoderms [13] exhibit lower calcification rates under the chemical conditions that are expected by the end of the century. However, some studies have found contradictory results (e.g. [14]).

Pteropods are among the calcifiers that are expected to be greatly affected by declining aragonite saturation state (Ω_a) (e.g. [15]). These macro-zooplankton are holoplanktonic molluscs that are widely distributed throughout all oceans. Their diel vertical migrations can cover several hundred metres. They are a major dietary component for some zooplankton and higher predators, such as herring, salmon, whales and birds, and they have an active role in the food web of pelagic ecosystems, particularly in high latitudes [16]. Pteropods are also major contributors to fluxes of calcium carbonate [17] and organic matter [18] to the deep ocean. It is expected that pteropods will be highly sensitive to these future changes in sea water chemistry, because they maintain an external calcareous shell made of aragonite [6,19,20], a relatively soluble form of calcium

* Author and address for correspondence: Department of Biology, California State University, 18111 Nordhoff Street, Northridge, CA 91330-8303, USA (steeve.comeau@csun.edu).
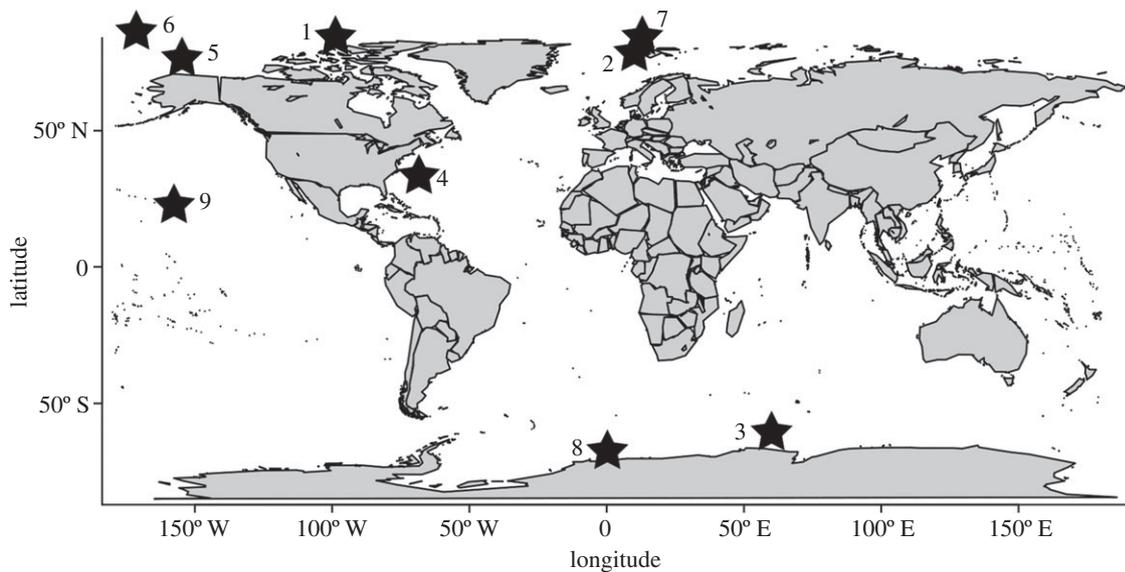
Figure 1. Location of the nine study sites.

Table 1. Study sites and corresponding vertical migration ranges for pteropods.

site	species	latitude	longitude	vertical migration (m)	reference
1	*L. helicina*	83.5° N	98.5° W	250	[24]
2	*L. helicina*	79° N	11° E	200	S. Comeau 2009, personal observation
3	*L. helicina*	62° S	60° E	200	[16]
4	*Creseis* sp.	33.5° N	69.5° W	150	[25]
5	*L. helicina*	74.5° N	154.5° W	250	[24]
6	*L. helicina*	84.5° N	171.5° W	250	[24]
7	*L. helicina*	82° N	11° E	150	[26]
8	*L. helicina*	68° S	0° E	200	[16]
9	*Creseis* sp.	21° N	158° W	200	[27]

carbonate [21]. Recent studies have demonstrated a strong relationship between the Ω_a and the rates of calcium carbonate precipitation in the Arctic pteropod species *Limacina helicina* [15,22] as well as the Mediterranean species *Creseis acicula* [23].

This study aims to link model projections for chemistry with laboratory data on pteropod calcification rates to estimate future changes in pteropod calcification. Thus, we combined model projections of future Ω_a with laboratory-derived empirical relationships relating gross calcification rates to Ω_a in order to estimate the *in situ* calcification rates of pteropods within the depth range of their vertical distribution.

2. MATERIAL AND METHODS

(a) *Data acquisition*

For our analysis, we chose sites having co-location of three types of data: (i) for the vertical distribution of pteropod species that have known responses of their calcification rate to the aragonite saturation state, (ii) for nearby carbonate chemistry, and (iii) for model projections of the aragonite saturation state projections. Data on the vertical migration of pteropods were obtained from six publications and one personal observation (table 1). These data provide information on vertical ranges of the high-latitude species *L. helicina* at five sites in the Arctic Ocean and two sites in the Southern Ocean (figure 1). Because the Arctic data from Kobayashi [24] covered a wide area, that dataset was divided into three

different sites. Additionally, data on another species, *C. acicula* were available at two study sites (Sargasso Sea and Hawaii). For simplicity, we consider that both species migrate vertically from the surface to 200 m, because vertical migrations at the different sites generally varied from 150 to 250 m for both *L. helicina* and *C. acicula*. For brevity, we have selected to provide details for two sites in the Arctic, one site in the Southern Ocean, and one site at temperate latitudes (sites 1–4, respectively). Particular attention was paid to the Arctic, the first region that is expected to become undersaturated with respect to aragonite [7]; it is also a region where pteropods play a major ecological role.

(b) *Institut Pierre Simon Laplace model*

Based on previous comparison efforts [6], differences between model projections over the next 100 years are relatively small after each model is corrected for its modern-day model-data bias. For simplicity, we used output from one Earth System Model (from Institut Pierre Simon Laplace, IPSL-CM4) forced under the IPCC SRES A2 scenario. Simulated fields of carbonate chemistry variables from the IPSL-CM4 model were used in this analysis. The climate system in this coupled model includes an atmospheric general circulation model (LMDZ4 [28]) that is coupled through the OASIS coupler to an ocean general circulation model (OPA8 [29]) that is itself coupled to a sea ice model (Louvain-la-Neuve ice model). Imbedded in this climate system are modules for the terrestrial biosphere (ORCHI-DEE [30]) and the marine carbon cycle (PISCES [31]).
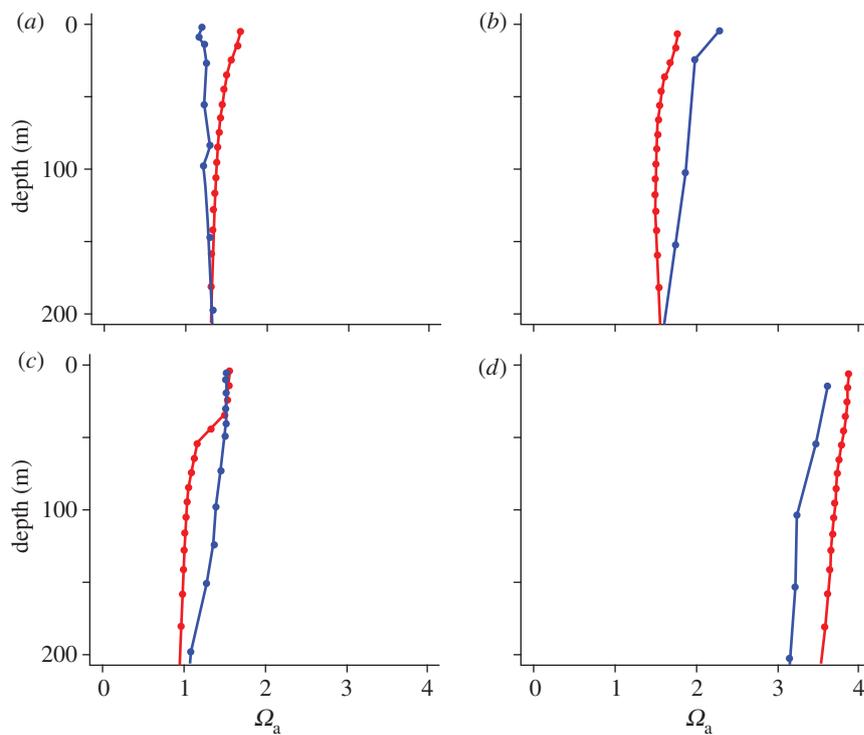
Figure 2. Aragonite saturation state (Ω_a) simulated by the model (red circles with solid line) and calculated from the field data (blue circles with solid line) for (*a*) study site 1 (Arctic Ocean; 83.5° N, 98.5° W), (*b*) study site 2 (Svalbard; 79° N, 11° E), (*c*) study site 3 (Southern Ocean; 62° S, 60° E) and (*d*) study site 4 (Sargasso Sea; 33.5° N, 69.5° W). Points on the colour curves indicate sample depths (blue) and model levels (red). A figure, similar to the one presented here, is available in the electronic supplementary material for the other study sites.

Table 2. Mean aragonite saturation state (Ω_a) ($\pm$ s.d.) from the model projections and the CARINA data over the top 200 m. (The symbol Δ represents the mean of the model minus that of the data over the top 200 m and the propagated error.)

site	longitude	latitude	model	data	Δ
1	98.5° W	83.5° N	1.39 ± 0.10	1.28 ± 0.04	0.11 ± 0.10
2	11° E	79° N	1.57 ± 0.07	1.92 ± 0.11	−0.35 ± 0.13
3	60° E	62° S	1.12 ± 0.21	1.37 ± 0.13	−0.26 ± 0.24
4	69.5° W	33.5° N	3.71 ± 0.10	3.33 ± 0.14	0.38 ± 0.17

More about the IPSL-CM4 Earth System Model and its validation can be found in Cadule *et al.* [32,33].

(c) Model correction
Data from stations in the CARINA database (CARbon IN the Atlantic [34]) nearest to the study sites were used both to evaluate present-day model behaviour and improved model projections. Observed total alkalinity (A_T), dissolved inorganic carbon (C_T), pressure, salinity, temperature and phosphate and silicate concentrations, collected between 2000 and 2005 depending on the site, were used to determine the corresponding Ω_a with the *R* package seacarb [35]. The calculated saturation states were then compared with model results from the same year. The model-minus-data difference, i.e. the model bias, was then subtracted following the approach of Orr *et al.* [6] in order to improve future projections.

(d) In situ *calcification*
The relationship between gross calcification (G_{gross}) and Ω_a for the Arctic pteropod *Limacina helicina helicina* ($G_{gross} = 0.57 \ln (\Omega_a) + 0.25$) was taken from Comeau *et al.* [15]; the relationship for the temperate pteropod *C. acicula*

($G_{gross} = 0.39 \ln (\Omega_a) + 0.3$) was taken from [23]. Known genetic differences between the Arctic pteropod *L. helicina helicina*, and the Antarctic pteropod *Limacina helicina antarctica* [36], were not considered for this analysis. Rates measured on Mediterranean species *C. acicula* were used in the two subtropical study sites, (Sargasso Sea and near Hawaii), where *C. acicula* is also found. As described in Comeau *et al.* [15], temperature effect was mainly reflected by its influence on the Ω_a. Relationships between $CaCO_3$ precipitation and Ω_a were not significantly different on pteropods incubated at 0°C and 4°C. Differences in temperature were then neglected. Annual-mean model output for the Ω_a was used to compute the corresponding G_{gross} *in situ*. Mean G_{gross} were calculated by assuming that pteropods migrate daily between the surface and 200 m. They are expressed in per cent relative to the estimated pre-industrial G_{gross}.

3. RESULTS
The projections of the IPSL model for the Ω_a are generally consistent with values derived from field measurements (figure 2, table 2 and electronic supplementary material,
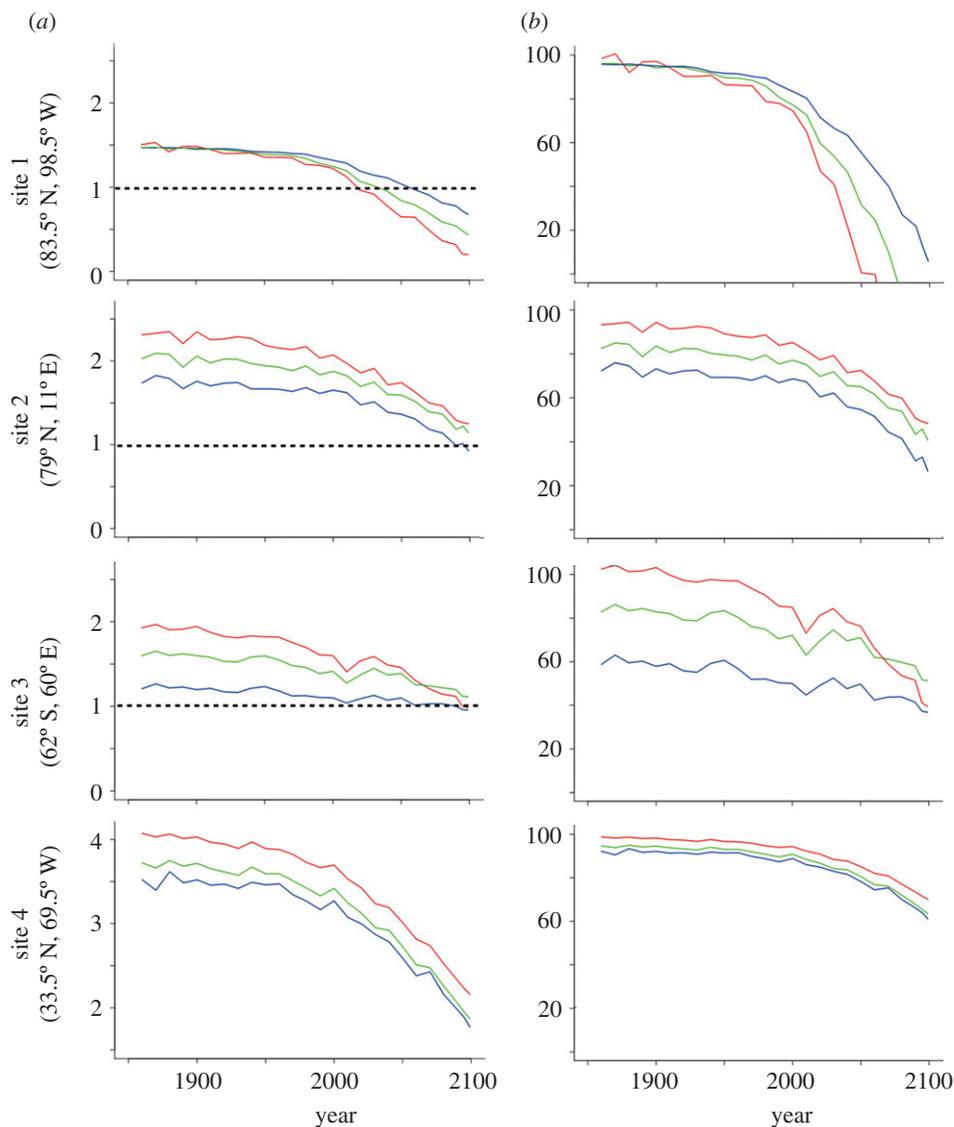
Figure 3. Mean annual aragonite saturation state (Ω_a) projected by the IPSL model (corrected for the modern model-data bias) during 1860–2100, and G_{gross} during 1860–2100 relative to the preindustrial rate at the four study sites. Lines are given for projections at 10 m (red), the mean over the 200 m vertical migration range (green) and at 200 m (blue). Dashed lines correspond to the limit between supersaturation and undersaturation with respect to aragonite. Site locations are given in the caption to figure 3. A figure, similar to the one presented here, is available in the electronic supplementary material for the other study sites. (a) Ω_a; (b) % of calcification.

figure S1). The mean of the model minus data for Ω_a over the top 200 m along with its propagated error are 0.11 ± 0.10, -0.35 ± 0.13, -0.26 ± 0.24 and 0.38 ± 0.17 at sites 1–4, respectively. The bias-corrected model projects that at site 1 in the Arctic, the mean Ω_a within the migration-depth range of pteropods was 1.5 in 1860, 1.2 in 2005, but only 0.4 at the end of the century (figure 3). On the west coast of Spitsbergen, at site 2, the mean Ω_a within the same depth range was 2.0 in 1860, 1.8 in 2005 and only 1.1 at the end of the century (figure 3). On an annual average, in the Arctic, these near-surface waters become undersaturated with respect to aragonite at all study sites by the end of the century (figure 3 and electronic supplementary material, figure S2). The decline is more pronounced at study site 1 (83.5° N, 98.5° W), where undersaturation with respect to aragonite is expected to occur over the top 200 m by 2050 (figure 3), relative to waters around Spitsbergen (site 2; 79° N, 11° E), where undersaturation is projected to occur only

by the end of the century (figure 3). In the Southern Ocean, site 3, the model projects that by 2100, the ASH will shoal to the surface, exposing pteropods to undersaturated waters throughout their range of vertical migration (figure 3). At that site, average Ω_a over the top 200 m is projected to decline from 1.6 in 1860 to 1.3 in 2005 and to drop to 1.1 by 2100. Temperate latitudes show larger absolute changes in Ω_a, but smaller relative changes: in the Sargasso Sea (site 4), near-surface Ω_a declines from 3.7 in 1860 to 1.9 in 2100, i.e. waters remain saturated in the pteropod vertical migration zone (figure 3).

Our calculations demonstrate that the projected reduction in Ω_a also greatly reduces pteropods gross calcification relative to pre-industrial rates, particularly in the high latitudes. In parts of the Arctic pteropods become unable to precipitate $CaCO_3$ during the second half of this century (figure 3 and table 3). Near Spitsbergen though, at the end of the century, pteropods still maintain some positive G_{gross} relative to preindustrial rate because

Table 3. Mean aragonite saturation state (Ω_a) projected by the model and corresponding G_{gross} rate relative to the pre-industrial value at each of the four study sites.

site	year	mean Ω_a	% of gross calcification relative to preindustrial
1 (Arctic)	1860	1.5	100
	2005	1.2	77
	2095	0.4	0
2 (Svalbard)	1860	2.0	100
	2005	1.8	92
	2095	1.1	50
3 (Antarctic)	1860	1.6	100
	2005	1.3	80
	2095	1.1	60
4 (Atlantic)	1860	3.7	100
	2005	3.3	95
	2095	1.9	67

Ω_a is naturally higher (figure 3). Nonetheless, at the same time and place, surface G_{gross} of *L. helicina* decline to 50 per cent of their preindustrial values while, G_{gross} at 200 m depth decline to 20 per cent of their preindustrial values. In the Southern Ocean, by the end of the century, the G_{gross} of *L. helicina* declines to 60 per cent of its preindustrial value (table 3). Southern Ocean G_{gross} were 40 per cent lower at 200 m than at the surface during preindustrial time, but in 2100, after the ASH has shoaled to the surface, differences throughout the 200 m migration zone are negligible (figure 3). At temperate latitudes (site 4), the G_{gross} in 2100 is projected to be approximately 70 per cent of the preindustrial rate (figure 3).

4. DISCUSSION

Our results suggest that high-latitude pteropods will be most affected by the anthropogenic decline in Ω_a, particularly in the Arctic. However, surface waters across the Arctic will experience different rates of change. For example, the Greenland Sea around Svalbard (site 2) will be less affected than the Arctic Ocean at site 1. This difference is explained by the different physical–chemical properties of the two areas. Svalbard waters are influenced by Atlantic water [37], with higher total alkalinity and temperature. The influence of Atlantic inflow in this area makes these waters less susceptible to undersaturation than those at higher latitudes (e.g. site 1). Generally though, Arctic pteropods appear to be particularly vulnerable to ocean acidification. One model study projects that undersaturation with respect to aragonite is expected to begin in 2016 over 10 per cent of the Arctic Ocean, for one month per year [7]. These low saturation zones will be associated with increased melting of ice and freshwater inputs leading to a decrease in total alkalinity [7]. Undersaturated conditions have already been found in near coastal waters under the influence of heavy freshwater influence [38].

Temperate latitudes showed large absolute changes in Ω_a, in the Atlantic (site 4, from $\Omega_a = 3.7$ in 1860 to $\Omega_a = 1.9$ in 2095) as well as in the Pacific (site 9, from $\Omega_a = 3.6$ in 1860 to $\Omega_a = 1.7$ in 2095). The situation is more critical in the North Pacific, where the shoaling of

the ASH is projected to reach the deepest portion of the migratory range of *Creseis* sp. by the end of the century (electronic supplementary material, figure S2), a consequence of the naturally much shallower ASH in the North Pacific [39]. The high-ratio dissolved inorganic carbon versus total alkalinity makes this area particularly vulnerable to ocean acidification [19].

The projected shoaling of less-saturated waters (figure 3) is also directly measurable in the field. In the Iceland Sea, measurements [40] demonstrate that the ASH is currently shoaling at a rate of 4 m yr^{-1}. This shoaling and the general reduction of Ω_a in near-surface waters will result in increased exposure of pteropods to less-saturated waters throughout their diurnal migrations. It is unknown if these changes in water chemistry could prompt pteropods to reduce their vertical migration length scale in order to reduce their exposure to less-saturated waters. Pteropods can be found as deep as 1200 m in some seasons [24], and thus may be already exposed to undersaturated waters during seasonal migration. At present, any such exposure must be limited in time. Although the exact reasons for these deep vertical migrations of pteropods and the associated physiological impacts are not known, zooplankton generally migrate diurnally or seasonally to reduce the predatory pressure [41]. Zooplankton typically feed near the surface, which is rich in food, but also in predators; they migrate to deeper layers to hide from their predators. For example, in the Kongsfjorden (Svalbard), juveniles of *L. helicina* overwinter at about 200 m and switch to feed on lower quality food [42,43]. If pteropods reduce their depth range in response to acidification or other anthropogenic pressures, that would also result in greater predatory pressure, notably on juveniles.

Our results highlight the critical situation that *L. helicina* will face in the coming decades in the Arctic Ocean. Moreover, these projections are conservative because they concern rate of G_{gross}, rather than rates of net calcification, which is the balance between G_{gross} and dissolution of calcium carbonate. Calcification rates were indeed measured using the ^{45}Ca incorporation technique [15], which estimates the active incorporation of $CaCO_3$ occurring mostly at the growing edge of the shell (aperture), but does not provide information about shell dissolution rates. In other words, even when pteropods precipitate $CaCO_3$ at the shell aperture, there may be simultaneous dissolution across the entire shell surface [23]. At some point, as G_{gross} declines and dissolution of $CaCO_3$ increases, rates of dissolution would become larger than rates of G_{gross} and net calcification would become negative.

In recent decades, as the Ω_a has declined, effects from corresponding reductions in pteropod calcification rate on abundance have yet to be detected. The 1951–2008 time series of zooplankton in Californian coastal waters reveals no evidence for declines in the abundance of *Thecosomata* pteropods [44], despite a measurable reduction of Ω_a in the same region [39]. Similar time series have not been investigated elsewhere.

To what extent might *Thecosomata* pteropods be able to survive without a shell? A laboratory study on larvae of the Mediterranean pteropod *Cavolinia inflexa* shows that larvae can be viable without a shell when they are reared in waters that are undersaturated with respect to aragonite [45]. Another study reports that larvae of the Arctic pteropods *L. helicina* are viable after 29 days of

laboratory incubation in waters that are undersaturated with respect to aragonite ($\Omega_a = 0.86$), although their shells exhibit extensive degradation [43]. We hypothesize that pteropod shells defend against small predators, such as small decapods, small medusa or small fish larvae, thus preventing them from feeding on shelled pteropods. Pteropods shells also offer their hosts a means to regulate their buoyancy and thus their diurnal migrations [46]. Moreover, for pteropod species of the order *Limacinadae*, the shell helps maintain the structural integrity of their soft body parts [45], which could make life without a shell unviable. We hypothesize that as the ocean warms and *L. helicina* migrate poleward, confined by its affinity for waters cooler than 5°C [47], it will be trapped by the shoaling aragonite horizon pushing pteropods nearer to equator. Throughout the northern oceans, *L. helicina* could thus disappear entirely by the end of the century after becoming incapable of calcifying enough to offset dissolution and other factors of shell erosion.

The loss of Arctic pteropods could have major biogeochemical, ecological and economic impacts. The potential impacts of their disappearance on fish populations and other predators, such as zooplankton, seabirds or whales will depend on the capacity of these predators to modify their diet. Fish populations could be affected from the bottom-up control of zooplankton, as already demonstrated regarding cod recruitment [48,49]. Another example is the potential impact on juvenile pink salmon, whose diet can consist of up to 60 per cent of *L. helicina* [50]. Without *L. helicina*, how would the required permanent switch to other prey of different nutritional value and abundance impact juvenile pink salmon? In any case, reductions in pink salmon, the most abundant salmon in the Pacific and the mainstay of North Pacific fisheries, would have major economic repercussions. Evaluating how the disappearance of pteropod populations would affect both economics and ecosystems remain as critical future research challenges.

We have provided regional estimates of the changes in pteropod calcification rates during the industrial era until the end of this century by linking model projections for chemical changes with laboratory data correlating those changes to pteropod calcification rates. More than ever, there appears little future for high-latitude shelled pteropods, particularly the dominant species *L. helicina*, assuming that atmospheric CO_2 continues to increase during the coming decades.

REFERENCES

1 Sabine, C. L. *et al.* 2004 The oceanic sink for anthropogenic CO_2. *Science* **305**, 367–371. (doi:10.1126/science. 1097403)

2 Meehl, G. A. & Stocker, T. F. 2007 Global climate projections. In *Climate Change 2007: the physical science basis. Contribution of Working Group I to the Fourth Assessment Report of the Intergovernmental Panel on Climate Change* (eds S. Solomon *et al.*), pp. 747–845. Cambridge, UK: Cambridge University Press.

3 Khatiwala, S., Primeau, F. & Hall, T. 2009 Reconstruction of the history of anthropogenic CO_2 concentrations in the ocean. *Nature* **462**, 346–349. (doi:10.1038/nature08526)

4 Caldeira, K. & Wickett, M. E. 2003 Oceanography: anthropogenic carbon and ocean pH. *Nature* **425**, 365. (doi:10.1038/425365a)

5 Leggett, J., Pepper, W. J. & Swart, R. J. 1992 Emissions Scenarios for the IPCC: an update. In *Climate Change 1992: The Supplementary Report to the IPCC Scientific Assessment* (eds J. T. Houghton, B. A. Callander & S. K. Varney), pp. 69–95. Cambridge, UK: Cambridge University Press.

6 Orr, J. C. *et al.* 2005 Anthropogenic ocean acidification over the twenty-first century and its impact on calcifying organisms. *Nature* **437**, 681–686. (doi:10.1038/nature04095)

7 Steinacher, M., Joos, F., Frölicher, T. L., Plattner, G. & Doney, S. C. 2009 Imminent ocean acidification in the Arctic projected with the NCAR global coupled carbon cycle-climate model. *Biogeosciences* **6**, 515–533. (doi:10. 5194/bg-6-515-2009)

8 Riebesell, U., Zondervan, I., Rost, B., Tortell, P. D., Zeebe, R. E. & Morel, F. M. M. 2000 Reduced calcification of marine plankton in response to increased atmospheric CO_2. *Nature* **407**, 364–367. (doi:10.1038/ 35030078)

9 Gattuso, J.-P., Allemand, D. & Frankignoulle, M. 1999 Photosynthesis and calcification at cellular, organismal and community levels in coral reefs: a review on interactions and control by carbonate chemistry. *Am. Zool.* **39**, 160–183. (doi:10.1093/icb/39.1.160)

10 Langdon, C. & Atkinson, M. J. 2005 Effect of elevated pCO_2 on photosynthesis and calcification of corals and interactions with seasonal change in temperature/ irradiance and nutrient enrichment. *J. Geophys. Res.* **110**, 1–16. (doi:10.200510.1029/2004JC002576)

11 Martin, S. & Gattuso, P. 2009 Response of Mediterranean coralline algae to ocean acidification and elevated temperature. *Glob. Change Biol.* **15**, 2089–2100. (doi:10.1111/j.1365-2486.2009.01874.x)

12 Gazeau, F., Quiblier, C., Jansen, J. M., Gattuso, J., Middelburg, J. J. & Heip, C. H. R. 2007 Impact of elevated CO_2 on shellfish calcification. *Geophys. Res. Lett.* **34**, (doi:10.1029/2006GL028554)

13 Dupont, S., Ortega-Martínez, O. & Thorndyke, M. 2010 Impact of near-future ocean acidification on echinoderms. *Ecotoxicology* **19**, 449–462. (doi:10.1007/s10646-010-0463-6)

14 Ries, J. B., Cohen, A. L. & McCorkle, D. C. 2009 Marine calcifiers exhibit mixed responses to CO_2-induced ocean acidification. *Geology* **37**, 1131–1134. (doi:10.1130/ G30210A.1)

15 Comeau, S., Jeffree, R., Teyssié, J.-L. & Gattuso, P. 2010 Response of the Arctic pteropod *Limacina helicina* to projected future environmental conditions. *PLoS ONE* **5**, e11362. (doi:10.1371/journal.pone.0011362)

16 Hunt, B., Pakhomov, E., Hosie, G., Siegel, V., Ward, P. & Bernard, K. 2008 Pteropods in southern Ocean ecosystems. *Prog. Oceanogr.* **78**, 193–221. (doi:10.1016/j. pocean.2008.06.001)

17 Honjo, S. 2004 Particle export and the biological pump in the Southern Ocean. *Antarct. Sci.* **16**, 501–516. (doi:10.1017/S0954102004002287)

18 Collier, R., Dymond, J., Honjo, S., Manganini, S., Francois, R. & Dunbar, R. 2000 The vertical flux of biogenic and lithogenic material in the Ross Sea: moored sediment trap observations 1996–1998. *Deep Sea Res. II* **47**, 3491–3520. (doi:10.1016/S0967-0645(00) 00076-X)

19 Feely, R. A., Sabine, C. L., Lee, K., Berelson, W., Kleypas, J., Fabry, V. J. & Millero, F. J. 2004 Impact of anthropogenic CO_2 on the $CaCO_3$ system in the oceans. *Science* **305**, 362–366. (doi:10.1126/science.1097329)

20 Fabry, V. J., Seibel, B. A., Feely, R. A. & Orr, J. C. 2008 Impacts of ocean acidification on marine fauna and ecosystem processes. *ICES J. Mar. Sci.* **65**, 414–432. (doi:10.1093/icesjms/fsn048)

21 Mucci, A. 1983 The solubility of calcite and aragonite in seawater at various salinities, temperatures, and one atmosphere total pressure. *Am. J. Sci.* **283**, 780–799. (doi:10.2475/ajs.283.7.780)

22 Comeau, S., Gorsky, G., Jeffree, R., Teyssié, J.-L. & Gattuso, P. 2009 Impact of ocean acidification on a key Arctic pelagic mollusc (*Limacina helicina*). *Biogeosciences* **6**, 1877–1882. (doi:10.5194/bg-6-1877-2009)

23 Comeau, S., Gattuso, J.-P., Jeffree, R. & Gazeau, F. Submitted. Effect of changes in the carbonate chemistry on calcification, respiration and excretion of a Mediterranean pteropod. *J. Plankton. Res.*

24 Kobayashi, H. A. 1974 Growth cycle and related vertical distribution of the thecosomatous pteropod *Spiratella* ('*Limacina*') *helicina* in the central Arctic Ocean. *Mar. Biol.* **26**, 295–301. (doi:10.1007/BF00391513)

25 Wormuth, J. H. 1981 Vertical distributions and diel migrations of Euthecosomata in the northwest Sargasso Sea. *Deep Sea Res.* **28**, 1493–1515. (doi:10.1016/0198-0149(81)90094-7)

26 Falk-Petersen, S. *et al.* 2008 Vertical migration in high Arctic waters during autumn 2004. *Deep Sea Res. II* **55**, 2275–2284. (doi:10.1016/j.dsr2.2008.05.010)

27 Nigro, D. T. & Seapy, R. R. 2008 Diel patterns of vertical distribution in Euthecosomatous pteropods of Hawaiian Waters. *Veliger* **50**, 190–209.

28 Hourdin, F. *et al.* 2006 The LMDZ4 general circulation model: climate performance and sensitivity to parametrized physics with emphasis on tropical convection. *Clim. Dyn.* **27**, 787–813. (doi:10.1007/s00382-006-0158-0)

29 Madec, G., Delecluse, P., Imbard, M. & Lévy, M. 1998 OPA 8.1 ocean general circulation model reference manual, 11, 91 pp. Notes du Pôle de Modélisation, Institut Pierre-Simon Laplace (IPSL), France.

30 Krinner, G., Viovy, N., De Noblet-Ducoudre, N., Ogee, J., Polcher, J., Friedlingstein, P., Ciais, P., Sitch, S. & Prentice, I. C. 2005 A dynamic global vegetation model for studies of the coupled atmosphere-biosphere system. *Glob. Biogeochem. Cyc.* **19**, GB1015. (doi:10.1029/2003GB002199)

31 Aumont, O. & Bopp, L. 2006 Globalizing results from ocean *in situ* iron fertilization studies. *Global Biogeochem. Cyc.* **20**, GB2017. (doi:10.1029/2005GB002591)

32 Cadule, P., Bopp, L. & Friedlingstein, P. 2009 A revised estimate of the processes contributing to global warming due to climate-carbon feedback. *Geophys. Res. Lett.* **36**, L14705. (doi:10.1029/2009GL038681)

33 Cadule, P., Bopp, L., Friedlingstein, P., Sitch, S., Jones, C. D., Ciais, P., Piao, S. L. & Peylin, P. 2010 Benchmarking coupled climate-carbon models against long-term atmospheric CO_2 measurements. *Global Biogeochem. Cyc.* **24**, GB2016. (doi:10.1029/2009GB003556)

34 Olsen, A. *et al.* 2009 Overview of the Nordic Sea's CARINA data and salinity measurements. *Earth Sys. Sci. Data* **1**, 25–34. (doi:10.5194/essd-1-252009)

35 Lavigne, H. & Gattuso, P. 2010 Seacarb: calculates parameters of the seawater carbonate system portions of code and/or corrections were contributed by Epitalon, J.-M., Gentili, B., Hofmann, A., Orr, J., Proye, A. & Soetaert, K. R package version 2.3.1. See http://CRAN.R-project.org/package=seacarb.

36 Hunt, B., Strugnell, J., Bednarsek, N., Linse, K., Nelson, R. J., Pakhomov, E., Seibel, B., Steinke, D. & Würzberg, L. 2010 Poles apart: the 'Bipolar' pteropod species *Limacina helicina* is genetically distinct between the Arctic & Antarctic Oceans. *PLoS ONE* **5**, e9835. (doi:10.1371/journal.pone.0009835)

37 Cottier, F., Tverberg, V., Inall, M., Svendsen, H., Nilsen, F. & Griffiths, C. 2005 Water mass modification in an Arctic fjord through cross-shelf exchange: the seasonal hydrography of Kongsfjorden, Svalbard. *J. Geophys. Res.* **110**, C12005. (doi:10.1029/2004JC002757)

38 Yamamoto-Kawai, M., McLaughlin, F. A., Carmack, E. C., Nishino, S. & Shimada, K. 2009 Aragonite undersaturation in the Arctic Ocean: effects of ocean acidification and sea ice melt. *Science* **326**, 1098–1100. (doi:10.1126/science.1174190)

39 Feely, R. A., Sabine, C. L., Hernandez-Ayon, J. M., Ianson, D. & Hales, B. 2008 Evidence for upwelling of corrosive 'acidified' water onto the Continental Shelf. *Science* **320**, 1490–1492. (doi:10.1126/science.1155676)

40 Olafsson, J., Olafsdottir, S. R., Benoit-Cattin, A., Danielsen, M., Arnarson, T. S. & Takahashi, T. 2009 Rate of Iceland Sea acidification from time series measurements. *Biogeosciences* **6**, 2661–2668. (doi:10.5194/bg-6-2661-2009)

41 Zaret, T. M. & Suffern, J. S. 1976 Vertical migration in zooplankton as a predator avoidance mechanism. *Limnol. Oceanogr.* **21**, 804–813. (doi:10.4319/lo.1976.21.6.0804)

42 Gannefors, C., Böer, M., Kattner, G., Graeve, M., Eiane, K., Gulliksen, B., Hop, H. & Falk-Petersen, S. 2005 The Arctic sea butterfly *Limacina helicina*: lipids and life strategy. *Mar. Biol.* **147**, 169–177. (doi:10.1007/s00227-004-1544-y)

43 Lischka, S., Büdenbender, J., Boxhammer, T. & Riebesell, U. 2010 Impact of ocean acidification and elevated temperatures on early juveniles of the polar shelled pteropod *Limacina helicina*: mortality, shell degradation, and shell growth. *Biogeoscie. Discuss.* **7**, 8177–8214. (doi:10.5194/bgd-7-8177-2010)

44 Ohman, M. D., Lavaniegos, B. E. & Townsend, A. W. 2009 Multi-decadal variations in calcareous holozooplankton in the California Current System: thecosome pteropods, heteropods, and foraminifera. *Geophys. Res. Lett.* **36**, L18608. (doi:10.200910.1029/2009GL039901)

45 Comeau, S., Gorsky, G., Alliouane, S. & Gattuso, P. 2010 Larvae of the pteropod *Cavolinia inflexa* exposed to aragonite undersaturation are viable but shell-less. *Mar. Biol.* **157**, 2341–2345. (doi:10.1007/s00227-010-1493-6)

46 Lalli, C. M. & Gilmer, R. W. 1989 *Pelagic snails. The biology of holoplanktonic gastropod mollusks*. Stanford, CA: Stanford University Press.

47 Chen, C. & Bé, A. W. 1964 Seasonal distributions of euthecosomatous pteropods in the surface waters of five stations in the Western North Atlantic. *Bull. Mar. Sci.* **14**, 185–220.

48 Beaugrand, G., Brander, K. M., Alistair Lindley, J., Souissi, S. & Reid, P. C. 2003 Plankton effect on cod recruitment in the North Sea. *Nature* **426**, 661–664. (doi:10.1038/nature02164)

49 Kirby, R., Beaugrand, G. & Lindley, J. 2009 Synergistic effects of climate and fishing in a marine ecosystem. *Ecosystems* **12**, 548–561. (doi:10.1007/s10021-009-9241-9)

50 Armstrong, J. L., Boldt, J. L., Cross, A. D., Moss, J. H., Davis, N. D., Myers, K. W., Walker, R. V., Beauchamp, D. A. & Haldorson, L. J. 2005 Distribution, size, and interannual, seasonal and diel food habits of northern Gulf of Alaska juvenile pink salmon *Oncorhynchus gorbuscha*. *Deep Sea Res. II* **52**, 247–265. (doi:10.1016/j.dsr2.2004.09.019)